Paull, C.K., Matsumoto, R., Wallace, P.J., and Dillon, W.P. (Eds.), 2000
Proceedings of the Ocean Drilling Program, Scientific Results, Vol. 164

22. HYDRATES ASSOCIATED WITH FLUID FLOW ABOVE SALT DIAPIRS (SITE 996)[1]

Per Kristian Egeberg[2]

ABSTRACT

Site 996 is located above the Blake Diapir where numerous indications of vertical fluid migration and the presence of hydrate existed prior to Ocean Drilling Program (ODP) Leg 164. Direct sampling of hydrates and visual observations of hydrate-filled veins that could be traced 30–40 cm along cores suggest a connection between fluid migration and hydrate formation. The composition of pore water squeezed from sediment cores showed large variations due to melting of hydrate during core recovery and influence of saline water from the evaporitic diapir below. Analysis of water released during hydrate decomposition experiments showed that the recovered hydrates contained significant amounts of pore water.

Solutions of the transport equations for deuterium (δ^2H) and chloride (Cl^-) were used to determine maximum (δ^2H) and minimum (Cl^-) in situ concentrations of these species. Minimum in situ concentrations of hydrate were estimated by combining these results with Cl^- and δ^2H values measured on hydrate meltwaters and pore waters obtained by squeezing of sediments, by the means of a method based on analysis of distances in the two-dimensional Cl^-–δ^2H space.

The computed Cl^- and δ^2H distribution indicates that the minimum hydrate amount solutions are representative of the actual hydrate amount. The highest and mean hydrate concentrations estimates from our model are 31% and 10% of the pore space, respectively. These concentrations agree well with visual core observations, supporting the validity of the model assumptions.

The minimum in situ Cl^- concentrations were used to constrain the rates of upward fluid migration. Simulation of all available data gave a mean flow rate of 0.35 m/k.y. (range: 0.125–0.5 m/k.y.).

INTRODUCTION

Clathrate hydrates of gas ("gas hydrates") are ice-like structures where cages of water molecules are stabilized by gas molecules (Sloan, 1990). Gas hydrates principally composed of CH_4 and water occur naturally in the pore space of marine sediment where appropriate high pressure and low-temperature conditions exist, and there is an adequate supply of methane (Kvenvolden, 1993).

The amounts of gas trapped in oceanic sediment gas hydrates (7.5 to 15×10^{18} g C as CH_4; Kvenvolden, 1988, 1993; MacDonald, 1990; Gornitz and Fung, 1994) comprise the Earth's largest fossil fuel reservoir. However, such global estimates must be regarded as speculative. Bottom-simulating reflectors (BSR's) have been interpreted as a phase boundary between overlying CH_4 hydrate and underlying free CH_4 gas for nearly three decades, but the amount and distribution of CH_4 in these two zones has been a long-standing and contentious issue (e.g., Shipley et al., 1979; Katzman et al., 1994; Wood et al., 1994; Holbrook et al., 1996; Paull, Matsumoto, Wallace, et al., 1996; Hovland et al., 1997).

On a local scale, measurements of pore-water Cl^- and the stable isotopes of oxygen (O) and hydrogen (H) on samples recovered from depth represent a potentially powerful method for quantifying gas hydrate amounts in marine sediment (Hesse, 1990; Hesse and Harrison, 1981). The use of these species for quantification of gas hydrate amounts is based on the fact that salts are excluded during hydrate formation, and the cage-building water molecules are enriched in the heavy isotopes O and H. The aqueous phase from which the hydrates form gets progressively enriched in salts and depleted in the heavy isotopes of O and H (Hesse, 1990). Hence, in closed systems the amounts of hydrate formed may be estimated from the Cl^- concentration and isotope signatures (H and O) of the surrounding pore water (Ussler and Paull, 1995).

However, hydrates decompose rapidly when the pressure is released during sampling. Thus, pore water extracted from hydrate-bearing sediments are usually mixtures of interstitial water and meltwater from the hydrates. Although quantification of gas hydrate amount from pore-water Cl^- and stable isotope measurements is conceptually simple, the method is not straightforward because in situ pore-water chemistry prior to gas hydrate dissociation is unknown. Estimates of gas hydrate amount made by this method, therefore, are entirely dependent on assumed in situ concentrations of Cl^-. Previous investigators (Kvenvolden and Kastner, 1990; Froelich et al., 1995; Kastner et al., 1995; Yuan et al., 1996) have assumed in situ pore-water Cl^- concentrations similar to that of seawater. As acknowledged by these authors, such an assumption neglects advection and diffusion of ions and results in overestimation of gas hydrate amount (Ussler and Paull, 1995). Until recently (Egeberg and Dickens, 1999), a paucity of information concerning fluid flow, in situ pore-water chemistry, and gas hydrate amount precluded alternative and better assumptions.

The aim of this work is to utilize the special conditions (upward migration of saline pore water) over the Blake Ridge Diapir to estimate the composition of the interstitial water (Cl^-, δ^2H), and to use these parameters to determine the amount of hydrates, based on analysis of pore water squeezed from whole-round cores and analysis of decomposed samples of hydrate.

ENVIRONMENTAL SETTING

The Blake Ridge Diapir is the southernmost in a series of about 20 diapiric structures rising from depth within sediments of the Carolina Trough near 32°30.5′N, 76°11.5′W, in a water depth of 2170 m (Fig. 1).

The Blake Ridge and adjacent Carolina Ridge are areas with BSRs. Seismic reflection profiles show that the BSR shoals from 0.5 to 0.3 s (two-way traveltime sub-bottom) over the crest of the Blake Ridge Diapir and that a small fault extends upward from the doming BSR to the seafloor over the diapir (Paull et al., 1995). Ocean Drilling

[1]Paull, C.K., Matsumoto, R., Wallace, P.J., and Dillon, W.P. (Eds.), 2000. *Proc. ODP, Sci. Results,* 164: College Station, TX (Ocean Drilling Program).
[2]Agder College, Tordenskjoldsgt. 65, 4604 Kristiansand, Norway.
per.k.egeberg@hia.no

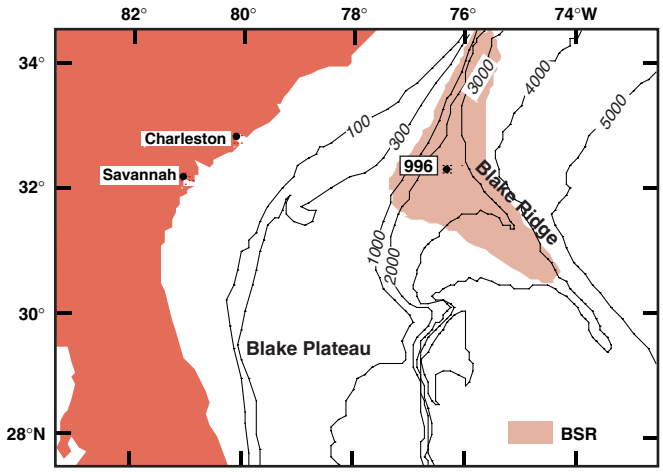

Figure 1. Map showing the location of ODP Site 996. Shaded region characterizes the portion of the Blake Ridge where geophysical evidence indicates the presence of a bottom-simulating reflector (BSR) and, by inference, zones of gas hydrate and underlying free gas (Dillon and Paull, 1983).

Program (ODP) Site 996 consisted of five holes that were located along a 80-m-long east–west transect across a mussel bed, which is presumably part of a chemosynthetic community fed by gas-charged fluids migrating along the fault system (Paull et al., 1995). Holes 996A, 996B, and 996C were located in this mussel bed. Holes 996D and 996E were 40 m to the east and west, respectively (Fig. 2).

The sedimentary sequence consists primarily of nannofossil-bearing clay and nannofossil-rich clay. Hard carbonate beds were encountered in two zones between 5 and 20 mbsf, and between 30 and 50 mbsf (Paull, Matsumoto, Wallace, et al., 1996). The maximum age of the recovered sediments is about 1.0 m.y. Gas hydrates were recovered from all five holes. The hydrates were white and occurred as massive pieces, platy fracture fillings, and vertically oriented rod-shaped nodules (Paull, Matsumoto, Wallace, et al., 1996).

MATERIAL AND METHODS

Twenty-two whole-round samples were taken for interstitial water analysis from Holes 996A (seven samples), 996D (six samples), and 996E (nine samples). The interstitial waters were extracted using the procedure and equipment described by Manheim and Sayles (1974). Eight samples of meltwater from dissociation experiments on massive pieces of hydrates were collected for analysis from Holes 996B (two samples of the same hydrate nodule), 996C (three samples of which two were taken from the same nodule), 996D (two samples), and 996E (one sample). Interstitial water and hydrate meltwater were analyzed for Cl^- (precision 0.2%) according to the methods described in ODP Technical Note 15 (Gieskes et al., 1991). The δ^2H values (reproducibility ± 0.5‰) were determined at Institute for Energy Technology (Kjeller, Norway) by reduction over Zn at 900°C and analysis of H_2 by a Finnigan MAT Delta E Isotope Ratio Mass Spectrometer. Values are reported relative to the standard mean ocean water (SMOW) scale.

RESULTS AND DISCUSSION

Cl^- Values

The Cl^- pore-water concentration profiles for Holes 996A, 996D, and 996E (Fig. 3) are characterized by a general increasing trend with increasing depth, and large fluctuations. Usually the concentration of Cl^- in pore waters from deep-sea sediments only vary by a few percent. At Site 996 the concentrations range from seawater values (560 mM) near the sediment/water interface to 970 mM at 54.26 mbsf in Hole 996E. The large variations are believed to be caused by varying amounts of hydrate decomposition during pore-water recovery and the influence of saline water from below. Many (possibly all) the pore-water samples are mixtures of hydrate meltwater and in situ pore water.

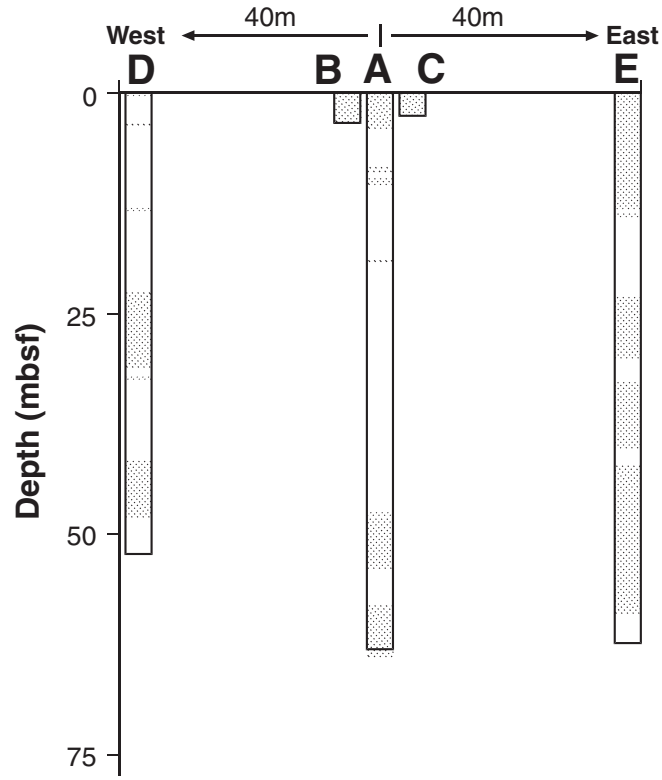

Figure 2. Location of Holes 996A, 996B, 996C, 996D, and 996E at Site 996 over the Blake Ridge Diapir (simplified from Paull, Matsumoto, Wallace, et al., 1996). Intervals of no recovery are blank. Note that the last core from Hole 996A is longer than the actually cored interval. The clam bed is situated above Holes 996A, 996B, and 996C.

Meltwater samples from pure hydrates should contain zero Cl^- concentrations because hydrates exclude ions during their growth. The concentration of Cl^- in the hydrate meltwaters range from 21 to 352 mM (Table 1); thus, all samples contain significant amounts of interstitial water. This is a common feature for hydrate samples from oceanic sediments (e.g., Kastner et al., 1990).

Numerous processes may produce subsurface brines in sedimentary sequences (e.g., Martin et al., 1995; Egeberg, 1992). In the present setting, the two most probable mechanisms are evaporite dissolution and ion exclusion by hydrate formation. The pronounced increase of the Na/Cl value with increasing depth (Paull, Matsumoto, Wallace, et al., 1996) strongly suggests that the interstitial water has acquired its high salinity by dissolution of evaporites and that the Blake Ridge Diapir is of evaporitic nature.

δ^2H Values

The δ^2H values of the pore-water samples range from –2‰ to 3.3‰ (Table 1) and show wide scattering when plotted vs. depth (Fig. 4).

Most pore-water profiles from deep-sea sediments show a progressive depletion in deuterium with depth below the seafloor (Friedman and Hardcastle, 1988). This has been attributed to glacial effects

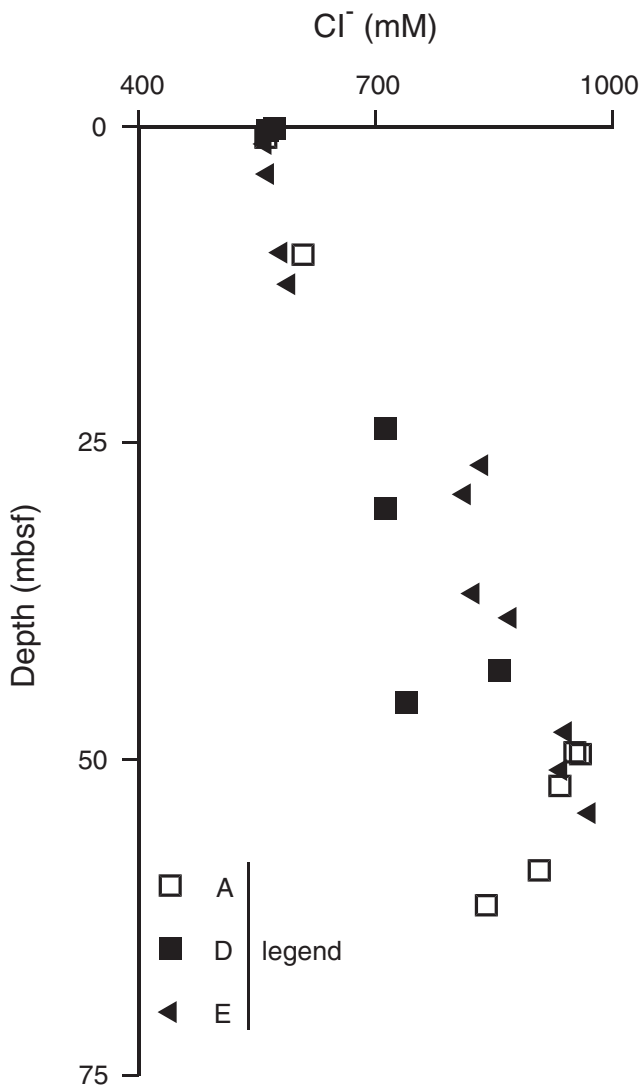

Figure 3. Measured concentrations of Cl^- in pore water squeezed from sediment cores from Holes 996A, 996D, and 996E.

(Friedman and Hardcastle, 1988), alteration of volcanic ash or basalts (Cole et al., 1987), dewatering of shales (Yeh, 1980), formation of hydrate (Kvenvolden and Kastner, 1990), and oxidation of mantle-derived methane and hydrogen (Lawrence and Taviani, 1988).

The hydrate meltwater samples are enriched in deuterium (range 8.1‰–17.1‰). The strongest heavy isotope enrichment is observed for Sample 164-996E-7H-CC, which contains only 21 mM Cl^-. For comparison, Kastner et al. (1990) reported δ^2H values of 19.3‰ and 17.6‰ for two hydrate samples containing 51.4 and 90.6 mM Cl^-, respectively. The first subsample of Core 164-996B-1H (2.1 mbsf) contains about 32% more Cl^- than the second subsample and is proportionally less enriched in deuterium (Table 1). The differences between the two subsamples of Core 164-996C-1H (2.3 mbsf) is about 16% in Cl^- and –12% in deuterium.

Evidence for Pore-Water Advection

Prior to Leg 164, Paull et al. (1995) had presented several evidences for pore-water advection at Site 996. The presence of a deep-sea chemosynthetic biological community suggests unusual conditions. These authors also observed high concentrations of CH_4 and H_2S in the shallow sediment cores and in the water column above,

Table 1. Measured and modeled concentrations of Cl^-, δ^2H, and estimated concentrations of hydrate for Site 996.

Core, section, interval (cm)	Depth (mbsf)	δ^2H (‰)	Cl^{-*} (mM)	$Cl^{-\dagger}$ (mM)	Hydrate (vol%)
Pore water samples:					
164-996A-					
1H-1, 85-95	0.85	0.4	561	576	2.5
3X-1, 61-71	10.11	1.9	608	703	13.5
8H-1, 96-111	49.46	–1.6	952	977	2.5
8H-2, 0-12	49.61	–1.1	959	1026	6.6
8H-5, 19-34	52.12	0.0	933	1086	14.1
9H-1, 80-90	58.8	0.3	907	1070	15.2
9H-3, 87-102	61.55	2.2	840	1177	28.6
164-996D-					
1H-1, 0-20	0.1	1.4	572	629	9.0
1H-1, 20-40	0.3	0.6	563	585	3.8
4H-2, 10-25	23.87	2.0	712	876	18.7
4H-7, 140-150	30.14	2.0	712	876	18.7
6H-2, 52-67	42.99	0.7	857	1018	15.8
6H-5, 28-43	45.49	3.3	739	1074	31.2
164-996E-					
1H-3, 72-87	3.72	0.6	563	585	3.8
2H-4, 134-150	9.94	0.7	580	610	4.9
2H-6, 117-132	12.44	2.4	590	704	16.2
4H-3, 135-150	26.75	–1.0	834	854	2.3
4H-5, 135-150	29.05	–1.1	812	819	0.9
5H-4, 135-150	36.9	0.5	823	942	12.6
5H-6, 72-87	38.82	0.5	870	1022	14.9
6X-4, 135-150	47.86	–1.5	940	967	2.8
7H-3, 10-19	54.26	–2.0	970	973	0.3
Hydrate samples:					
164-996B-					
1H-3	2.1	10.4	248	612	57.7
1H-3	2.1	13.8	169	612	76.4
164-996C-					
1H-CC	2.3	9.2	294	612	48.9
1H-CC	2.3	10.3	245	612	55.3
2H-CC	2.4	8.1	352	612	44.4
164-996D-					
2X-CC	3.5	13.5	139	600	75.4
5X-CC	32.1	12.9	317	988	70.1
164-996E-					
7H-CC	58.63	17.1	21	974	99.1

Note: * = measured, † = simulated.

and acoustically defined water-column plumes that apparently emanate from a fault connecting the seafloor to the base of the BSR.

Direct sampling of hydrates during Leg 164 confirms that pore waters at Site 996 contain concentrations of CH_4 sufficient to stabilize hydrates. This is unexpected for sediments with moderate organic carbon concentrations (0.41%, n = 14), and suggest influx of CH_4 from below. Gas hydrate–filled veins that were 1–3 mm thick and could be traced 30–40 cm along cores represent possible flow conduits. Numerous veins similar to these are probably closely spaced in the sediments because two parallel veins were observed in an individual core and because veins were found in most of the cores below 30 mbsf.

Estimation of Hydrate Amount

Egeberg and Dickens (1999) showed that the amount of hydrate and rate of fluid migration may be determined by solving the transport equations for two conservative pore-water constituents, provided the concentrations of these species in pore waters squeezed from hydrate-free sediments (sediments from below the BSR) have been determined. At Site 996 the BSR was not penetrated; hence an alternative method is used here. The method used for estimating the amount of hydrate is based on the assumption that the rate of exchange of pore water by fluid migration is so rapid that formation of hydrates and other diagenetic reactions do not influence the concentration of pore-water Cl^- and deuterium. This assumption will be discussed below when discussing the source of water and gas.

In situ concentration profiles of Cl^- and deuterium are generated by the model included in Appendix A. The concentration profiles are

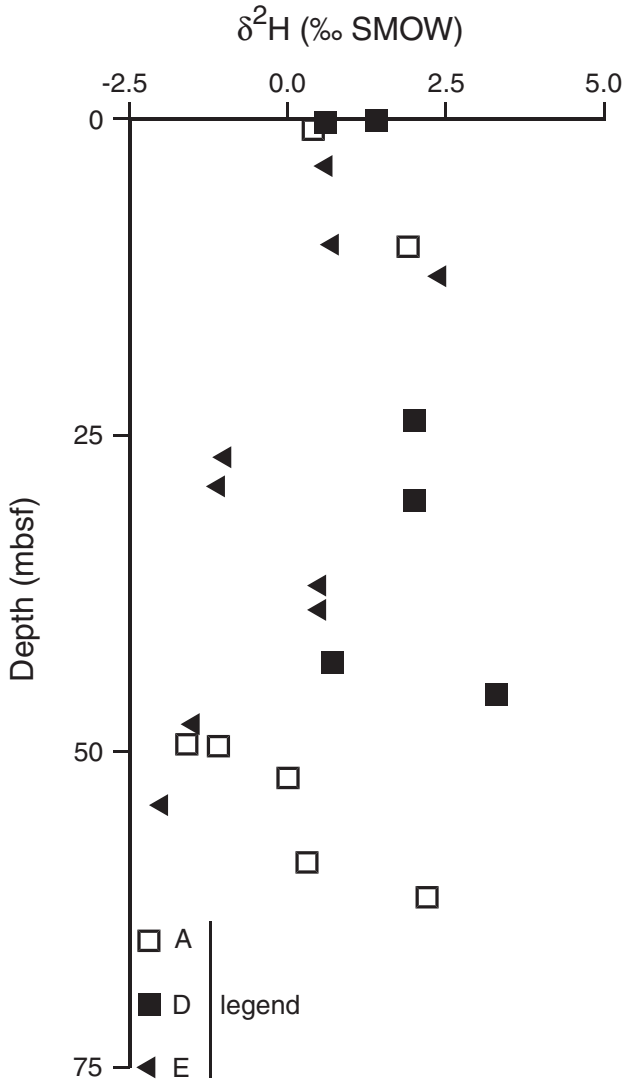

Figure 4. Measured δ^2H values in pore water squeezed from sediment cores from Holes 996A, 996D, and 996E.

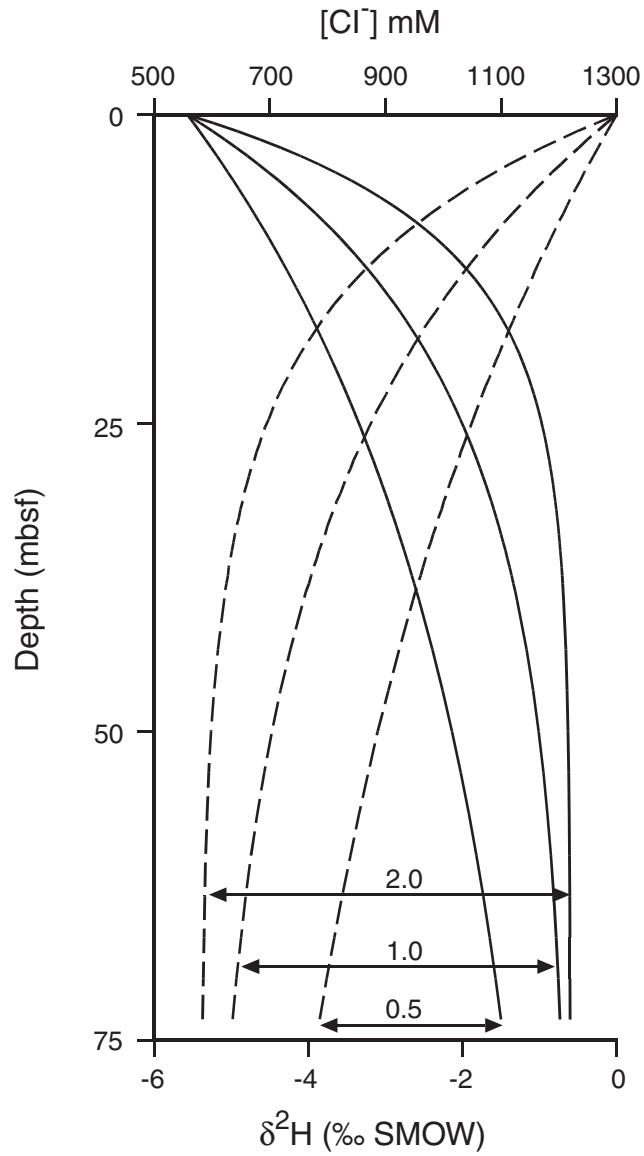

Figure 5. **A.** Solutions of the transport equations (Appendix A) for Cl^- (solid curves) and δ^2H (dashed curves) for three different rates of upward pore-water migration (0.5, 1.0, and 2.0 m/k.y.).

very sensitive to the assumed rate of pore-water advection (Fig. 5A). However, when the simulated δ^2H values are plotted vs. the simulated Cl^- concentrations, this flow-rate dependency vanishes (Fig. 5B).

The fact that the flow-rate dependency vanishes when the concentrations of one conservative dissolved species are plotted vs. the concentrations of a second conservative species is the basis for the method of estimating the hydrate amount used here. The flow-rate independent curve (Figs. 5B, 6) will be referred to as the FRI-curve.

Actual pore-water compositions should plot at the FRI-curve if the sediment from which the pore-water sample was obtained did not contain hydrate. Pore-water samples diluted by meltwater from hydrates should plot above the FRI-curve, because hydrates are enriched in deuterium (Fig. 6).

The distance from the FRI-curve provides a measure of the amount of hydrate meltwater in a pore-water sample and may be used for quantification. The difficult part is to determine the input parameters for constructing the FRI-curve, which is the lower boundary conditions for modeling of the in situ Cl^- and δ^2H profiles. Seawater values for Cl^- (560 mM) and δ^2H (0‰ SMOW) are assumed for the upper boundary conditions. Because all of the recovered pore-water samples may be diluted by hydrate meltwater, the lower boundary Cl^- concentration must be higher or equal to the highest measured Cl^- concentration (970 mM, Table 1), and the lower boundary δ^2H value must be more negative or equal to the most negative measured δ^2H value (–2.0‰ SMOW, Table 1). However, there is no lower constraint on the FRI-curve (Fig. 6). Minimum estimates of the amount of hydrate may be obtained by choosing lower boundary conditions, which results in a FRI-curve that intersects the most negative δ^2H value. One set of lower boundary conditions that fulfill this condition when the lower boundary is set at 250 mbsf is 1400 mM Cl^-, –5.6‰ SMOW (curve 1, Fig. 6). It is possible to construct similar curves with other lower boundary conditions, for example 1600 mM Cl^-, –6.4‰ SMOW. However this uncertainty has no effect on hydrate amount estimates because the distances between the measurements and the FRI-curve remain the same.

The procedure for estimating hydrate amount is described in Appendix B. The hydrate-amount estimates (Fig. 7) suggest the presence of hydrates immediately below the seafloor in all holes.

Shallow occurrence of hydrate is consistent with the observation of massive pieces of hydrates in the first core from Holes 996B,

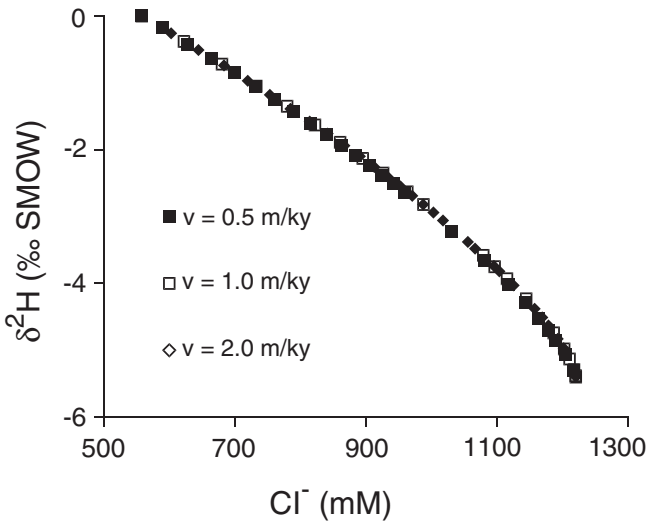

Figure 5 (continued). **B.** Data from Part A. The flow-rate dependency vanishes when the concentrations of two conservative pore-water constituents are combined. This type of curve is referred to as FRI-curve in the text (flow-rate independent curve).

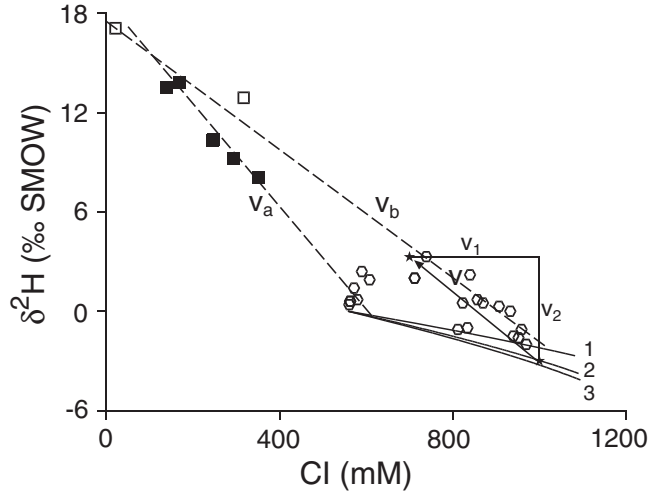

Figure 6. Measured pore-water (open hexagons) compositions and hydrate meltwater compositions for samples from depths shallower than 3.5 mbsf (filled squares) and greater than 32 mbsf (open squares). Curves labeled 1, 2, and 3 are FRI-curves determined with lower boundary conditions, with [Cl^-] and δ^2H of 1400 and –5.6, 1220 and –5.6, and 1220 and –6.0, respectively. The principle for determination of hydrate amount (see Appendix B) is demonstrated by vector V, which shows how the composition of a pore-water sample with an initial composition on FRI-curve 2 will change when mixed with hydrate meltwater. The slope of vector V can be calculated from the initial composition of the pore water (Appendix B). Hydrate amount is determined by decomposition of the vector V that intersects a particular pore-water or hydrate meltwater composition into vectors V_1 and V_2. Vector V_a was used to determine the composition of the shallow hydrate samples. The composition of the deepest hydrate sample was determined by the means of vector V_b.

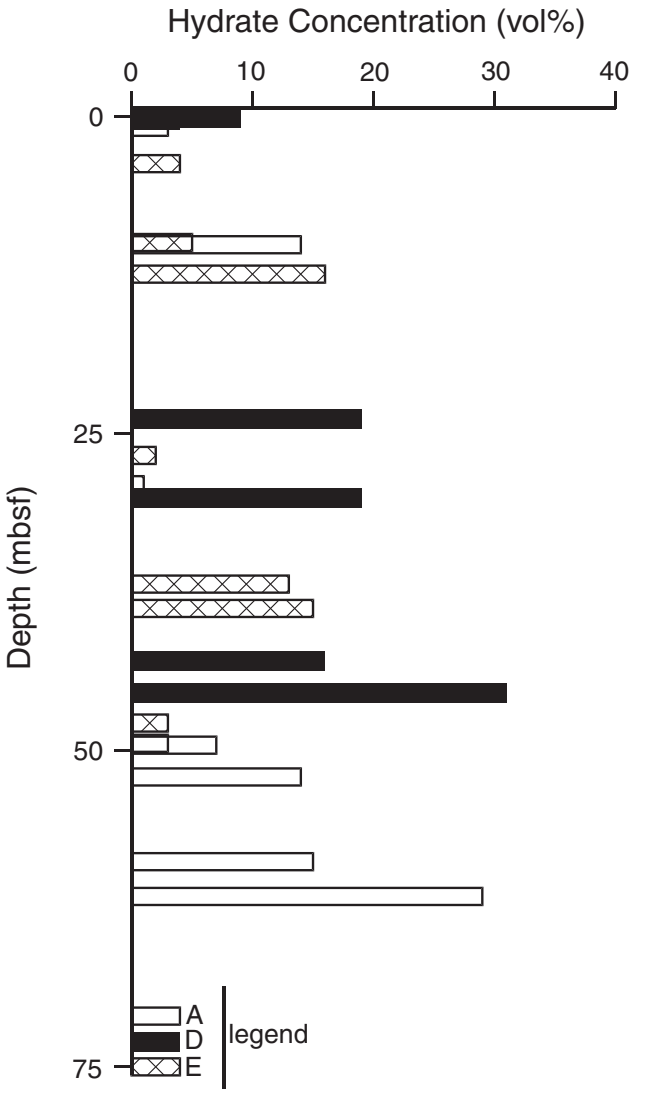

Figure 7. Distribution of hydrate in Holes 996A, 996D, and 996E determined by the method described in the caption of Figure 6.

996C, and 996D. The first two cores from Hole 996A were left for over an hour to degas H_2S before splitting, and no visual observations of their hydrate content could be made (Paull, Matsumoto, Wallace, et al., 1996). In Hole 996E, the first visual detection of gas hydrate was made in Core 164-996E-4H (23.2–32.7 mbsf). Recovery was extremely low (3.8%) for Core 164-996E-3X. In Cores 164-996A-9H and 164-996D-6H, which contain the highest theoretical estimates of hydrate amount (29% and 31% respectively), hydrates were observed as wavy, approximately vertical veins as much as 0.5 cm thick and 3–4 cm wide that could be traced about 30–40 cm along the cores. The mean hydrate concentration in the sampled sequence is 10% of pore space. As explained above, this is a minimum estimate because there is no lower constraint on the FRI-curve (Fig. 6). However, the fact that several samples plot close to the selected FRI-curve (i.e., several samples do not contain hydrate) does suggest that the selected curve is the most probable, because visual core observations did reveal a patchy distribution of hydrate. Hence, it seems unlikely that all samples taken for pore-water squeezing contained hydrate.

All samples of hydrate meltwaters contain appreciable concentrations of Cl^- and are less enriched in deuterium than one would expect for marine hydrates (e.g., Kastner et al. 1990), because the hydrate samples are contaminated by pore water. Estimates of the amounts of hydrate in these samples range from 44% to 99% (Table 1). Note that because the vectors used to estimate the amounts of hydrate in the hydrate samples intersects at low Cl^- concentrations (Fig. 6), the solutions are not unequivocal. However, it is possible to choose the correct solution if one also considers the sample depths, because the in

situ Cl^- concentration must increase with increasing depth. Hence, the composition of the shallow (2.1–3.5 mbsf) hydrate samples (filled squares) was determined by means of vector V_a, and the composition of the deep hydrate samples (32.1 and 58.63 mbsf, Table 1), as determined by vector V_b (Fig. 6).

Estimation of Rates of Fluid Migration

Estimation of rates of fluid migration is based on the estimates of in situ Cl^- from above (Table 1) by adjusting the advection term in the transport equation (Appendix A) until the simulated Cl^- concentrations match the data.

It is evident that all data cannot be fitted with a single flow rate (Fig. 8). This is not surprising because the permeability field is probably quite heterogeneous because of the presence of fractures and carbonate-cemented layers (Paull, Matsumoto, Wallace, et al., 1996). Most of the data can be fitted with upward flow rates between 0.125 and 0.5 m/k.y. These flow rates are one to two orders of magnitude greater than pore-water flow rates generated by sediment compaction. Nevertheless, they seem too low to sustain the benthic biological community and are difficult to reconcile with the observations of water-column plumes (Paull et al., 1995). However, the derived flow rates must be regarded as averages for the whole diapir cross section, and the flow rates may be considerably larger on a local scale (i.e., along faults; see "Influence of the Fracture System" section, this paper).

Quantification of fluid flow is important, because it may help explain the shallow occurrence of hydrate at Site 996. An elegant model to account for formation of hydrate in organic-poor sediments involves recycling of CH_4 by gas bubbles rising across the BSR (e.g., Paull et al., 1994). According to this model, most of the hydrate growth should occur close to the BSR. At Site 996 the BSR is located at ~250 mbsf (estimated from Paull et al. (1995), fig. 1). It is evident from direct observations and hydrate amount estimates presented here that prevailing conditions at Site 996 allow formation of hydrate at much shallower depth, despite the low content of organic matter.

At Site 996 vein-filling hydrates were recovered from several cores (Paull, Matsumoto, Wallace, et al., 1996), supporting the hypothesis that formation of massive hydrates is associated with fluid advection. Other models for the formation of natural gas hydrate differ from Paull et al. (1994) in that they involve active fluid flow (e.g., Soloviev and Ginsburg, 1994; Hyndman and Davis, 1992; Egeberg and Dickens, 1999) rather than rising CH_4 bubbles.

The rate of pore-water flow at the nearby ODP Site 997 has been estimated to be about 0.2 m/k.y. (Egeberg and Dickens, 1999). The sediments at Site 997 contain a mean hydrate concentration of 2.3% (Egeberg and Dickens, 1999). At Site 996 the mean flow rate is 0.35 m/k.y., and the mean hydrate concentration is about 10% of pore space. Based on chlorinity data, Hyndman and Davis (1992) estimated a mean hydrate concentration at Deep Sea Drilling Project (DSDP) Sites 496 and 497 (lower and mid-slope of the Pacific active margin off Guatemala respectively) of about 25%, in association with a upward rate of fluid migration of 1 m/k.y. Similar calculations for the northern Cascadian accretionary ridge showed that a hydrate layer of up to 100 m thickness may form in response to a rate of fluid expulsion of 3 m/k.y.

Vertical advection of fluids promote precipitation of hydrates at shallow depth by two effects. First, it provides a supply of CH_4 that might otherwise not be sufficient to saturate the pore water with respect to hydrates in organic-poor sediments. Second, it provides a mechanism to reduce the concentration of sulfate and thereby allow concentrations of CH_4 to build up, both by increasing the rate of sulfate reduction via methane-oxidizing bacteria (e.g., Borowski et al., 1996) and by counteracting diffusion of seawater sulfate into the sequence. At Site 996 significant concentrations of sulfate (>1 mM) were not observed below 7 mbsf in any core (Paull, Matsumoto, Wallace, et al., 1996), similar to Site 892 at Cascadia where there is also seafloor seepage and a bioherm present (Kastner et al., 1995).

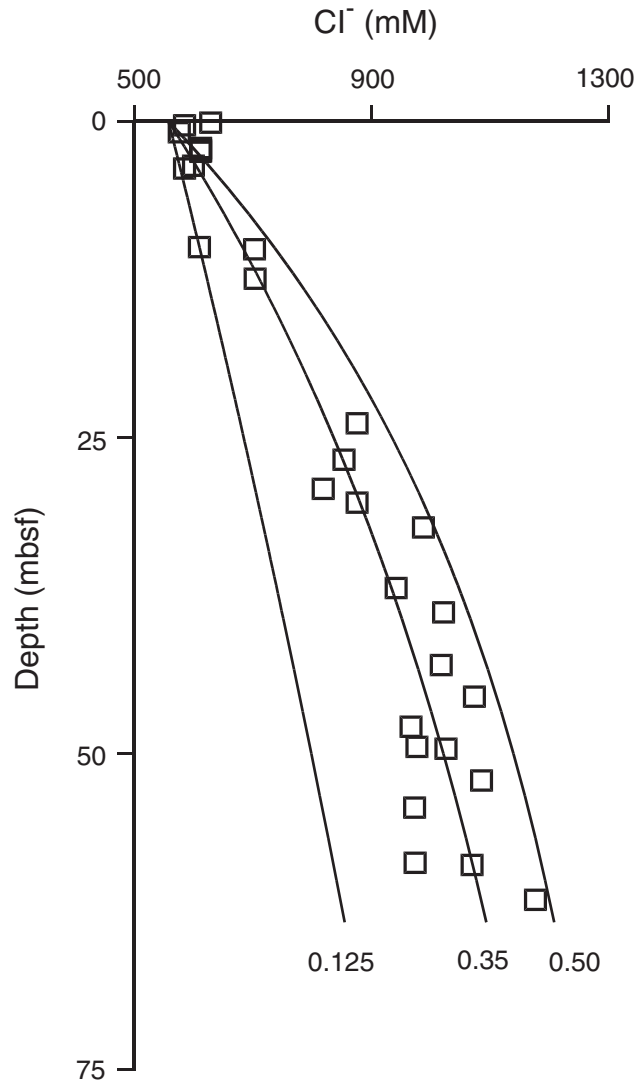

Figure 8. Solutions of the transport equation for Cl^- used to constrain the rate of upward pore-water migration between 0.125 and 0.5 m/k.y.

Source of Water and Gas

It has been suggested previously that decomposition of hydrates below the BSR may be the source of advecting fluids and gas at the Blake Ridge Diapir (Paull et al., 1995). Using a rate of sediment accumulation of 0.066 m/k.y., a concentration of hydrate of 10%, and a porosity of 50% result in an estimated rate of burial of hydrate-bound H_2O of about 3.1 kg/m^2/k.y. When the hydrate-bearing sediments are buried across the BSR and melt, this meltwater may contribute to the upward advective flux of pore fluids. However, the flow rates derived by modeling of the Cl^- data gives a total advective pore-water flux of 60–250 kg/m^2/k.y. Hence, the proportion of hydrate meltwater in the ascending pore water is probably not more than a few percent; most of the ascending pore water must come from another source than melting of hydrate. The best-fit lower boundary conditions (1400 mM Cl^-, –5.6‰ δ^2H) are consistent with this finding. If hydrate melt-

water constitutes a significant proportion of the ascending pore water, one would expect heavy δ^2H values and low Cl^- concentration. We believe that the source of the ascending water is pore water from the sedimentary sequences surrounding the Blake Ridge Diapir. By using the rate of sedimentation for Site 996 as an estimate for the regional rate of sedimentation, a rate of burial of pore water of about 30 $kg/m^{-2}/k.y.$ in regions without externally induced pore-fluid flow is estimated. Hence, the water budget for the diapir may be balanced by assuming that pore water is focused towards the diapir from a surrounding area that is 2–8 times greater than the area of the diapir itself. On the other hand, if one assumes that hydrate meltwater is the main source of the ascending water (Paull et al., 1995), then the drainage area would have to be 20–80 times greater than the area of the diapir, which seems less realistic. We suggest that the local high rate of pore-fluid flow at Site 996 is caused by focusing of pore water from a larger area by the structures created by the rising diapir. Paull et al. (1995) proposed that gas and fluid flow may be focused laterally towards the diapir along a permeable conduit beneath the base of a gas hydrate seal. However, if free gas does exist below the BSR, as suggested by Dickens et al. (1997) for other Leg 164 sites, then this zone will be characterized by low water permeability because of the reduced cross section available for pore-water flow.

Parts of the CH_4 incorporated into hydrates may come from CH_4 released during decomposition of hydrates below the BSR and advected upward (recycling). The CH_4 flux associated with the burial of hydrate (28 $mol/m^2/k.y.$) is of the same order of magnitude as the advective flux of dissolved CH_4 (11–43 $mol/m^2/k.y.$, assuming a saturation concentration of 170 mM). However, an unknown amount of dissolved CH_4 is discharged across the sediment/water interface and is not available for formation of hydrate. Hence, it seems that simple recycling of CH_4 from the BSR is not sufficient to balance the CH_4 budget. Furthermore, an additional amount of CH_4 is required to also balance the sulfate budget, because CH_4 is consumed by sulfate reducing bacteria with a 1:1 stoichiometry (Borowski et al., 1996). Due to large spatial variations in the sulfate gradient, it is difficult to estimate the size of the sulfate flux. The steepest sulfate gradient (Core 164-996D-1H, –266 mMm^{-1}) gives a sulfate flux of approximately 1600 $mol/m^2/k.y.$, whereas the lowest sulfate gradient (Hole 996E, –4 mMm^{-1}) gives a sulfate flux of 20 $mol/m^2/k.y$. Although we can not accurately estimate the apparent CH_4 deficiency, it may amount to several tens to hundreds of $mol/m^2/k.y.$ Methanogenesis of dissolved organic carbon supplied by the ascending pore water and internal CH_4 generation from sedimentary organic matter are the most likely sources of the missing CH_4. Egeberg and Barth (1998) reported concentrations of nonvolatile dissolved organic carbon (DOC) of up to 95 mM in the ascending pore water from the nearby Site 997. Conversion of this amount of carbon would add another 6–24 $mol/m^2/k.y.$ to the supply of CH_4. Pore waters from Site 996 have not been analyzed for DOC. The flux of sedimentary organic carbon is about 18 $mol/m^2/k.y.$ (rate of sedimentation 66 m/m.y.; porosity: 70%; concentration of organic carbon: 0.4%, Paull, Matsumoto, Wallace, et al., 1996). Hence, internal generation of CH_4 from sedimentary organic carbon is restricted to a few $mol/m^2/k.y.$, because only a fraction of the sedimentary organic matter can be microbiologically converted to CH_4 (Henrichs and Reeburgh, 1987).

Mass balance calculations may also be used to justify the fundamental assumption made in this study that the system is transport dominated, rather than reaction dominated with respect to Cl^- and deuterium. A system is transport dominated if the flux of dissolved species through the system is several times larger than the rates of diagenetic reactions that may influence the concentration of the species. The distinction is important because modeling of transport-dominated systems does not require incorporation of reaction terms into the diagenetic equation. The rate of exclusion of Cl^- by formation of hydrate (3 $mol/m^2/k.y.$) derived from the rate of burial of hydrate (3.4 $kg/m^2/k.y.$) and a pore-water Cl^- concentration of 1000 mM constitutes only a small fraction of the flux of Cl^- through the sequence (60–250 $mol/m^2/k.y.$). Similar calculations for deuterium give similar results; the fluxes of these components through the system are one to two orders of magnitude higher than the integrated rates of hydrate formation. Hence, the assumption of a transport dominated system seems to be valid because no other diagenetic reaction is known that could possibly affect the concentration of these species at this level.

Influence of the Fracture System

The model used to estimate the pore-water advection rates (Appendix A) assumes diffusion and advection through a homogeneous porous matrix and does not explicitly handle flow through fractures, although the presence of vein-like hydrates in cores indicates that most of the flow takes place through the closely spaced fracture system. The validity of using this model under the present conditions may be judged from the following considerations. The time required for molecular diffusion to eliminate concentration gradients between the highly permeable fracture system and the blocks of sediments between the fractures is probably small compared to the vertical component of the pore-water advection velocity. For example, for a fracture spacing of 10 cm, 90% of the concentration difference is eliminated by molecular diffusion in less than 0.13 yr (Fig. 9).

Note that the time required to homogenize the concentration field is independent of the magnitude of the concentration gradient, because large concentration gradients cause large mass fluxes per unit time. The time required to eliminate the difference in concentration between fractures and a sediment block increases by the square of the block dimensions, but it only takes about 13 yr to eliminate 90% of a concentration difference for a fracture spacing of 100 cm. Even this is short compared to the residence time of water in the sequence (>150 k.y). Based on the core observations, the fracture spacing is probably on a centimeter rather than a meter scale; hence it seems likely that the interstitial water is always close to equilibrium with the water flowing through the fractures. Therefore, the model probably generates valid results, even if it does not include fracture flow.

CONCLUSIONS

Simultaneous solution of the transport equations for pore-water Cl^- and δ^2H may be used to construct characteristic curves that are independent of the assumed rate of pore-water migration. Minimum in situ concentrations of hydrate can be determined by combining these curves with the results of Cl^- and δ^2H measurements on water from hydrate decomposition experiments and pore water obtained by squeezing of sediments, provided the system is transport dominated. This is not a serious restriction because formation of hydrate in deep-sea sediments seems to be closely associated with fluid flow. The method, which is based on analysis of distances in the two-dimensional Cl^-–δ^2H space, generates in situ Cl^- concentrations that may be used to estimate rates of fluid flow. It is also possible to evaluate whether the minimum hydrate-amount estimates are representative of the actual hydrate concentrations by considering the distribution of pore-water compositions relative to the characteristic curves.

At Site 996 this method results in hydrate concentrations from 0% to 31% of pore space, with a mean hydrate concentration of 10%. The highest hydrate concentration was determined for cores with visual detection of hydrate-filled veins as much as 0.5 cm thick and 3–4 cm wide that could be traced about 30–40 cm along the cores.

The rate of upward fluid migration could be constrained to 0.125–0.5 m/k.y., with a mean value of 0.35 m/k.y. Mass balance calculations showed that decomposition of hydrate below the BSR is insuf-

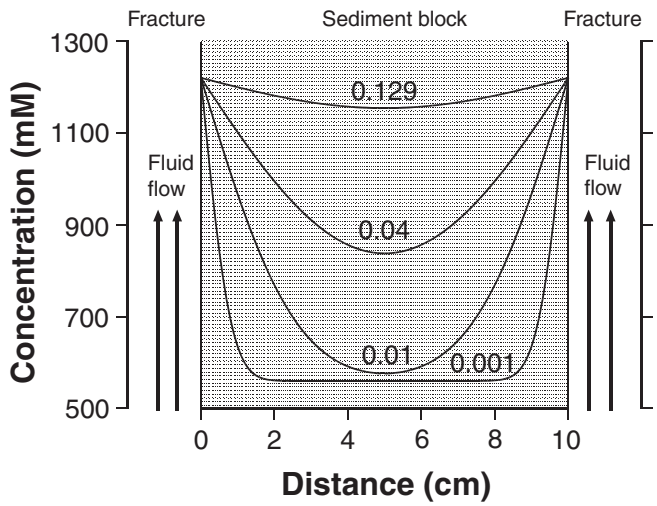

Figure 9. The figure is generated by means of the model (Appendix A) to demonstrate the time required for the pore water in a 10-cm-wide sediment block (porosity = 0.6, temperature = 25°C) to equilibrate with water in the surrounding fracture system. Initial conditions: C(0,x) = 560 mM; boundary conditions: C(t,0) = C(t,10) = 1220 mM. The curves show the concentration of Cl^- at 0.001, 0.01, 0.04, and 0.129 yr after a brine with a Cl^- concentration of 1220 mM started flowing through the fracture system.

ficient to account for the fluxes of water and CH_4, and that the fluxes of Cl^- and H_2O are one to two orders of magnitude higher than the integrated rates of hydrate formation.

ACKNOWLEDGMENTS

I thank C. Paull, R. Matsumoto, and P. Wallace for organizing the remarkably successful expedition, and A. Pimmel and T. Bronk in the *JOIDES Resolution* chemistry laboratory for their careful work. This work was funded by the Norwegian Research Council.

REFERENCES

Borowski, W.S., Paull, C.K., and Ussler, W., III, 1996. Marine pore-water sulfate profiles indicate in situ methane flux from underlying gas hydrate. *Geology,* 24:655–658.

Cole, D.R., Mottl, M.J., and Ohmoto, H., 1987. Isotopic exchange in mineral-fluid systems, II. Oxygen and hydrogen isotopic investigation of the experimental basalt-seawater system. *Geochim. Cosmochim. Acta,* 51:1523–1538.

Dickens, G.R., Paull, C.K., Wallace, P., and the ODP Leg 164 Scientific Party, 1997. Direct measurement of in situ methane quantities in a large gas-hydrate reservoir. *Nature,* 385:427–428.

Dillon, W.P., and Paull, C.K., 1983. Marine gas hydrates, II. Geophysical evidence. *In* Cox, J.L. (Ed.), *Natural Gas Hydrates: Properties, Occurrences, and Recovery:* Woburn, MA (Butterworth), 73–90.

Egeberg, P.K., 1992. Brines in sedimentary environments. *In* Yelles, M. (Ed.), *Encyclopedia of Earth System Science* (Vol. 1): London (Academic Press), 395–407.

Egeberg, P.K., and Barth, T., 1998. Contribution of dissolved organic species to the carbon and energy budgets of hydrate bearing deep sea sediments (Ocean Drilling Program Site 997 Blake Ridge). *Chem. Geol.,* 149:25–35.

Egeberg, P.K., and Dickens, G.R., 1999. Thermodynamic and pore water halogen constraints on gas hydrate distribution at ODP Site 997 (Blake Ridge). *Chem. Geol.,* 153:53–79.

Friedman, I., and Hardcastle, K., 1988. Deuterium in interstitial water from deep-sea cores. *J. Geophys. Res*., 96:8249–8263.

Froelich, P.N., Kvenvolden, K.A., Torres, M.E., Waseda, A., Didyk, B.M., and Lorenson, T.D., 1995. Geochemical evidence for gas hydrate in sediment near the Chile Triple Junction. *In* Lewis, S.D., Behrmann, J.H., Musgrave, R.J., and Cande, S.C. (Eds.), *Proc. ODP, Sci. Results,* 141: College Station, TX (Ocean Drilling Program), 279–286.

Gieskes, J.M., Gamo, T., and Brumsack, H., 1991. Chemical methods for interstitial water analysis aboard *JOIDES Resolution. ODP Tech. Note,* 15.

Gornitz, V., and Fung, I., 1994. Potential distribution of methane hydrates in the world's oceans. *Global Biogeochem. Cycles,* 8:335–347.

Greenspan, D., and Casulli, V., 1988. *Numerical Analysis for Applied Mathematics, Science, and Engineering:* Redwood City (Addison-Wesley).

Harris, K.R., and Woolf, L.A., 1980. Pressure and temperature dependence of the self diffusion coefficient of water and oxygen-18 water. *J.C.S. Faraday I,* 76:377–385.

Henrichs, S.M., and Reeburgh, W.S., 1987. Anaerobic mineralization of marine sediment organic matter: rates and the role of anaerobic processes in the oceanic carbon economy. *J. Geomicrobiol.,* 5:191–237.

Hesse, R., 1990. Pore-water anomalies in gas hydrate-bearing sediments of the deeper continental margins: facts and problems. *J. Inclusion Phenom. Mol. Recognit. Chem.,* 8:117–138.

Hesse, R., and Harrison, W.E., 1981. Gas hydrates (clathrates) causing pore-water freshening and oxygen isotope fractionation in deep-water sedimentary sections of terrigenous continental margins. *Earth Planet. Sci. Lett.,* 55:453–462.

Holbrook, W.S., Hoskins, H., Wood, W.T., Stephen, R.A., Lizzarralde, D., and the Leg 164 Science Party, 1996. Methane gas-hydrate and free gas on the Blake Ridge from vertical seismic profiling. *Science,* 273:1840–1843.

Hovland, M., Gallagher, J.W., Clennell, M.B., and Lekvam, K., 1997. Gas hydrate and free gas volumes in marine sediments: example from the Niger Delta front. *Mar. Pet. Geol.*, 14:245–255.

Hyndman, R.D., and Davis, E.E., 1992. A mechanism for the formation of methane hydrate and seafloor bottom-simulating reflectors by vertical fluid expulsion. *J. Geophys. Res.,* 97:7025–7041.

Kastner, M., Elderfield, H., Martin, J.B., Suess, E., Kvenvolden, K.A., and Garrison, R.E., 1990. Diagenesis and interstitial-water chemistry at the Peruvian continental margin—major constituents and strontium isotopes. *In* Suess, E., von Huene, R., et al., *Proc. ODP, Sci. Results,* 112: College Station, TX (Ocean Drilling Program), 413–440.

Kastner, M., Kvenvolden, K.A., Whiticar, M.J., Camerlenghi, A., and Lorenson, T.D., 1995. Relation between pore fluid chemistry and gas hydrates associated with bottom-simulating reflectors at the Cascadia Margin, Sites 889 and 892. *In* Carson, B., Westbrook, G.K., Musgrave, R.J., and Suess, E. (Eds.), *Proc. ODP, Sci. Results,* 146 (Pt 1): College Station, TX (Ocean Drilling Program), 175–187.

Katzman, R., Holbrook, W.S., and Paull, C.K., 1994. A combined vertical incidence and wide-angle seismic study of a gas hydrate zone, Blake Outer Ridge. *J. Geophys. Res.,* 99:17975–17995.

Kvenvolden, K.A., 1988. Methane hydrate—a major reservoir of carbon in the shallow geosphere? *Chem. Geol.,* 71:41–51.

————, 1993. Gas hydrates: geological perspective and global change. *Rev. Geophys.,* 31:173–187.

Kvenvolden, K.A., and Kastner, M., 1990. Gas hydrates of the Peruvian outer continental margin. *In* Suess, E., von Huene, R., et al., *Proc. ODP, Sci. Results,* 112: College Station, TX (Ocean Drilling Program), 517–526.

Lawrence, J.R., and Taviani, M., 1988. Extreme hydrogen, oxygen, and carbon isotope anamolies in the pore waters and carbonates of the sediments and basalts from the Norwegian Sea: methane and hydrogen from the mantle? *Geochim. Cosmochim. Acta,* 52:2077–2084.

Lehmann, M., and Siegenthaler, U., 1991. Equilibrium oxygen- and hydrogen-isotope fractionation between ice and water. *J. Glaciol.*, 37:23–26.

MacDonald, G.J., 1990. Role of methane clathrates in past and future climates. *Clim. Change,* 16:247–281.

Manheim, F.T., and Sayles, F.L., 1974. Composition and origin of interstitial waters of marine sediments, based on deep sea drill cores. *In* Goldberg, E.D. (Ed.), *The Sea* (Vol. 5): *Marine Chemistry: The Sedimentary Cycle:* New York (Wiley), 527–568.

Manheim, F.T., and Waterman, L.S., 1974. Diffusimetry (diffusion constant estimation) on sediment cores by resistivity probe. *In* von der Borch, C.C., Sclater, J.G., et al., *Init. Repts. DSDP,* 22: Washington (U.S. Govt. Printing Office), 663–670.

Martin, J.B., Kastner, M., and Egeberg, P.K., 1995. Origins of saline fluids at convergent margins. *In* Taylor, B., and Natland, J. (Eds.), *Active Margins*

and Marginal Basins of the Western Pacific. Geophys. Monogr., Am. Geophys. Union, 88:219–239.
McDuff, R.E., and Ellis, R.A., 1979. Determining diffusion coefficients in marine sediments: a laboratory study of the validity of resistivity techniques. *Am. J. Sci*., 279:666–675.
Out, D.J.P., and Los, J.M., 1980. Viscosity of aqueous solutions of univalent electrolytes from 5 to 95°C. *J. Sol. Chem*., 9:19–35.
Paull, C.K., Matsumoto, R., Wallace, P.J., et al., 1996. *Proc. ODP, Init. Repts.,* 164: College Station, TX (Ocean Drilling Program).
Paull, C.K., Ussler, W., III, and Borowski, W.A., 1994. Sources of biogenic methane to form marine gas-hydrates: in situ production or upward migration? *Ann. N.Y. Acad. Sci.,* 715:392–409.
Paull, C.K., Ussler, W., III, Borowski, W.S., and Spiess, F.N., 1995. Methane-rich plumes on the Carolina continental rise: associations with gas hydrates. *Geology*, 23/1:89–92.
Rard, J.A., and Miller, D.G., 1979. The mutual diffusion coefficients of NaCl–H_2O and $CaCl_2$–H_2O at 25°C from Rayleigh Interferometry. *J. Sol. Chem.,* 8:701–716.
Shipley, T.H., Houston, M.H., Buffler, R.T., Shaub, F.J., McMillen, K.J., Ladd, J.W., and Worzel, J.L., 1979. Seismic evidence for widespread possible gas hydrate horizons on continental slopes and rises. *AAPG Bull.,* 63:2204–2213.
Sloan, E.D., 1990. *Clathrate Hydrates of Natural Gases:* New York (Marcel Dekker).
Soloviev, V., and Ginsburg, G.D., 1994. Formation of submarine gas hydrates. *Bull. Geol. Soc. Den.,* 41:86–94.
Ussler, W., III, and Paull, C.K., 1995. Effects of ion exclusion and isotopic fractionation on pore water geochemistry during gas hydrate formation and decomposition. *Geo-Mar. Lett.,* 15:37–44.
Wood, W.T., Stoffa, P.L., and Shipley, T.H., 1994. Quantitative detection of methane hydrate through high-resolution seismic velocity analysis. *J. Geophys. Res.,* 99:9681–9695.
Yeh, H.-W., 1980. D/H Ratios and late-stage dehydration of shales during burial. *Geochim. Cosmochim. Acta*, 44:341–352.
Yuan, T., Hyndman, R.D., Spence, G.D., and Desmons, B., 1996. Seismic velocity increase and deep-sea gas hydrate concentration above a bottom-simulating reflector on the northern Cascadia Continental Slope. *J. Geophys. Res.,* 101:13655–13671.

Date of initial receipt: 27 April 1998
Date of acceptance: 10 March 1999
Ms 164SR-218

APPENDIX A

Diagenetic models for the dissolved constituents (Na, Cl, and deuterium) take the same form.

The flux of Cl^- is governed by

$$F_{Cl} = -DP\frac{\partial C}{x} + VPC, \tag{A1}$$

where C (concentration of Cl^-), D (diffusion coefficient), P (porosity), and V (rate of pore-water flow relative to sediment/water interface) may be functions of time and depth. The diffusion coefficient is described as a function of pore-water viscosity (η) and sediment tortuosity (τ) as

$$D = D_0\left(\frac{\eta_0}{\eta}\right)\tau^{-2}. \tag{A2}$$

D_0 is the diffusion coefficient at a reference temperature T_0 at which the viscosity of the pore water is η_0. The temperature dependence of η is taken from Out and Los (1980) for 0.7 molal NaCl solutions. The tortuosity term (McDuff and Ellis, 1979) is approximated by

$$\tau^2 = PF, \tag{A3}$$

where F (formation factor) is expressed as an exponential function of pore space (P),

$$F = P^{-n}, \tag{A4}$$

with n = 1.8 (average value for deep-sea sediments, Manheim and Waterman, 1974).

Assuming steady-state porosity conditions, the rate of flow of pore water is described by:

$$V = \frac{P^\infty}{P}(W^\infty + Va^\infty), \tag{A5}$$

where P^∞, W^∞, and Va^∞ are porosity, rate of particle flux relative to the sediment surface, and externally induced rate of pore-water flow relative to the sediment/water interface at the depth of fully compacted sediment, respectively. W^∞ is calculated from

$$W^\infty = s\frac{1-P^0}{1-P^\infty}. \tag{A6}$$

The principle of conservation of mass gives

$$\frac{\partial(PC)}{\partial t} = -\frac{\partial - F_{Cl}}{\partial x}. \tag{A7}$$

The partial differential equation is solved by the upwind Crank-Nicolson formula (e.g., Greenspan and Casulli, 1988).

The diffusion coefficient for HDO was assumed equal to that of H_2O (Harris and Woolf, 1980). The Cl^- was modeled by means of the diffusion coefficient for NaCl(aq), which changes by less than 1.1% over the range of concentrations encountered here (Rard and Miller, 1979).

APPENDIX B

The method for determination of hydrate amount is based on Figure 6 and the assumptions of isotopic equilibrium between pore water and hydrate and 100% exclusion of Cl^- during formation of hydrate.

First, values for the concentration of Cl^- and δ^2H are assigned to the ascending brine and the transport equations (Appendix A) are used to generate flow-rate-independent curves (FRI-curves, see "Estimation of Hydrate Amount" section, this paper) using these values as boundary conditions (curves labeled 1, 2, and 3 in Fig. 6). The FRI-curves represent all possible combinations of in situ pore-water Cl^- concentrations and δ^2H values ($[Cl^-]_{pw}$ and δ^2H_{pw}) for the chosen boundary conditions.

Second, a vector V is constructed that starts from the FRI-curve ($[Cl^-]_{pw}$, δ^2H_{pw}) and projects into the $[Cl^-]$–δ^2H space with a slope given by

$$\frac{\partial(\delta^2H)}{\partial[Cl^-]} = -\frac{(\delta^2H_{pw} + 1000)(\alpha - 1)}{[Cl^-]_{pw}}, \tag{B1}$$

where α is the isotope fractionation factor between hydrate and water.

This vector represents the change in $[Cl^-]$ and δ^2H that takes place when pore water with an initial composition given by the point ($[Cl^-]_{pw}$, δ^2H_{pw}) on the FRI-curve is diluted by hydrate meltwater. This is justified as follows.

Measured concentrations of Cl^- and δ^2H ($[Cl^-]_m$, δ^2H_m) are volumetric averages of pore-water compositions ($[Cl^-]_{pw}$, δ^2H_{pw}) and hydrate meltwater compositions (0, δ^2H_H),

$$[Cl^-]_m = f \cdot 0 + (1-f)[Cl^-]_{pw} \text{ and} \tag{B2}$$

$$\delta^2H_m = f\delta^2H_H + (1-f)\delta^2H_{pw}, \tag{B3}$$

where f is the volume fraction of hydrate meltwater. Because of the assumption of isotopic equilibrium, δ^2H_H and δ^2H_{pw} are related through:

$$\alpha = \frac{\delta^2H_H + 1000}{\delta^2H_{pw} + 1000}. \tag{B4}$$

Following the example of Kvenvolden and Kastner (1990) the hydrogen isotope fractionation factor for the hydrate-water system is set equal to the

fractionation factor for the ice-water system (1.021, Lehmann and Siegenthaler, 1991).

By evaluating

$$\frac{\partial f}{\partial [Cl^-]_m} \tag{B5}$$

from Equation B2, and

$$\frac{\partial (\delta^2 H_m)}{\partial f} \tag{B6}$$

from Equations B3 and B4, the slope of the vector may be derived from:

$$\frac{\partial (\delta^2 H_m)}{\partial [Cl^-]_m} = \frac{\partial (\delta^2 H_m)}{\partial f} \frac{\partial f}{\partial [Cl^-]_m} = -\frac{(\delta^2 H_{pw} + 1000)(\alpha - 1)}{[Cl^-]_{pw}}. \tag{B7}$$

Third, the starting point of the vector V is moved along the FRI-curve until it intersects a measured pore water or hydrate sample composition (Fig. 6). This step is repeated until each measured point is represented by a vector.

Fourth, the vector V is decomposed into the vectors v_1 and v_2 (Fig. 6) which provides an estimate of the amount of hydrate based on the measured Cl^- concentrations and δ^2H values respectively.